

RESEARCH

Open Access



Engineering *Saccharomyces cerevisiae* for the production of dihydroquercetin from naringenin

Shiqin Yu^{1,2,3,4}, Mingjia Li^{1,2,3,4}, Song Gao and Jingwen Zhou^{1,2,3,4*}

Abstract

Background: Dihydroquercetin (DHQ), a powerful bioflavonoid, has a number of health-promoting qualities and shows potential as a treatment for a number of disorders. Dihydroquercetin biosynthesis is a promising solution to meet the rising demand for dihydroquercetin. However, due to the significant accumulation of eriodietylol (ERI), naringenin (NAR), dihydrokaempferol (DHK), and other metabolites, the yield of DHQ biosynthesis is low. As a result, this is the hindrance to the biosynthesis of DHQ.

Results: In this study, we proposed several strategies to enhance the product formation and reduce the metabolites in accumulation. The flavonoid 3'-hydroxylase (F3'H) and cytochrome P450 reductase from different species were co-expressed in *S. cerevisiae*, and the best strain expressing the P450-reductase enzyme complex (*SmF3'H/ScCPR*) yielded 435.7 ± 7.6 mg/L of ERI from NAR in the deepwell microplate. The product conversion rate was improved further by mutating the predicted potential ubiquitination sites to improve *SmF3'H* stability, resulting in a 12.8% increase in titre using the mutant *SmF3'H* (K290R). Besides, different F3Hs from various sources and promoters were tested for the improved DHQ production, with the best strain producing 381.2 ± 10.7 mg/L of DHQ from 1 g/L of NAR, suggesting the temporal regulation the expression of F3H is important for maximization the function of F3'H and F3H.

Conclusion: This study offers effective strategies for improving DHQ production from NAR and could be used as a reference for related research.

Keywords: Dihydroquercetin, Bioproduction, *Saccharomyces cerevisiae*, Naringenin

Introduction

Dihydroquercetin, commonly known as taxifolin, is a bioactive flavonoid found in plants such as milk thistle, red onion, and acai palm, as well as in various commercial preparations like Legalon, Pycnogenol, and Venoruton [1, 2]. DHQ has two stereocenters and four types of stereoisomers: (+)-taxifolin, (–)-taxifolin, (+)-epitaxifolin, and (–)-epitaxifolin; and these stereoisomers have different activities and distribution in the body [3]. The

biological activities of dihydroquercetin, such as antioxidation, antiviral, and anticancer, render it an important dietary supplement and functional food, offering therapeutic promise in some disease prevention and treatment, such as neurodegenerative diseases, hypertension, and viral infection [2, 3]. Studies have shown that the antioxidant capacity of dihydroquercetin surpasses that of common antioxidants such as tocopherols and ascorbic acid, which is a powerful free radical neutraliser that protects body tissues from harmful free radicals [4]. In both in vivo and in vitro tests, dihydroquercetin has been shown to be effective as a cancer treatment via multiple mechanisms with little or no side effects on normal healthy cells [5]. In recent years, dihydroquercetin has

*Correspondence: zhoujw1982@jiangnan.edu.cn

¹ Science Center for Future Foods, Jiangnan University, 1800 Lihu Road, Wuxi 214122, Jiangsu, China
Full list of author information is available at the end of the article



© The Author(s) 2022. **Open Access** This article is licensed under a Creative Commons Attribution 4.0 International License, which permits use, sharing, adaptation, distribution and reproduction in any medium or format, as long as you give appropriate credit to the original author(s) and the source, provide a link to the Creative Commons licence, and indicate if changes were made. The images or other third party material in this article are included in the article's Creative Commons licence, unless indicated otherwise in a credit line to the material. If material is not included in the article's Creative Commons licence and your intended use is not permitted by statutory regulation or exceeds the permitted use, you will need to obtain permission directly from the copyright holder. To view a copy of this licence, visit <http://creativecommons.org/licenses/by/4.0/>. The Creative Commons Public Domain Dedication waiver (<http://creativecommons.org/publicdomain/zero/1.0/>) applies to the data made available in this article, unless otherwise stated in a credit line to the data.

been shown as a promising inhibitor for coronaviruses by inhibiting 3C-like protease [6], and it may be used as an efficient free radical scavenger in the treatment of COVID-19 in the near future [7]. As the need for an effective medicine with few or no side effects grows, this substance has come to light as a possible way to produce better medicine to meet the growing demand.

Currently, DHQ is commonly extracted from the wood of Dahurian Larch, but this tree grows slowly as it thrives in the world's most northern region, where climatic circumstances are exceptionally harsh [8]. Extraction from plant materials is a typically tedious process involving the use of toxic organic solvents [8–10]. Chemical synthesis of (\pm)-taxifolin has been documented, and requires chiral reverse-phase HPLC for chiral separation [11]. Although around 25% of marketed drugs are racemic mixtures, the single-isomer has significant therapeutic importance since one of the isomers could provide more effective treatment, high bioavailability, lower exposure in poor metabolizers, and less interindividual variation [12, 13]. As compared to chemical synthesis, bioproduction is more suited to producing such structurally complicated natural chemicals that involve stereoselectivity, and customers prefer products labelled with "bio". DHQ can be stereospecifically hydroxylating at the C-ring of ERI at the 3'-position or the B-ring of DHK at the 3-position by the enzyme flavanone 3-hydroxylase (F3H), and both of these molecules can be synthesized from NAR, an inexpensive starting material that could be extracted from the fruit-juice industry's wastes [14]. *Yarrowia lipolytica* was engineered to produce 110.5 mg/L of DHQ from glucose while also accumulating a significant amount of metabolites, including 252.4 mg/L of NAR and 134.2 mg/L of ERI [15]. Recently, the *Escherichia coli* was engineered to convert 100 mg/L of NAR to 13.6 mg/L of DHQ, and the bacterium was further engineered to produce 20.1 mg/L of DHQ from glycerol with a significant accumulation of DHK and NAR [16]. These studies have shown that DHQ can be bioproduced via the key metabolite NAR by further hydroxylation at specific positions, but future research should focus on addressing the problem of significant mediator accumulations and the low yield of target compound.

Previous research has shown that flavonoid 3'-hydroxylase (F3'H) and flavanone 3-dioxygenase (or flavanone 3-hydroxylase, F3H) are rate-limited steps in NAR hydroxylation [15–17], with F3'H requiring cytochrome P450 reductase for electron transfer. Many F3'Hs and F3Hs have been mined and functionally analyzed [18–21], but no systematic comparison of the activities involved in DHQ production has been conducted. Previous studies have also shown that the optimization of the expression of enzyme and its redox partner could

lead to a substantial improvement in product formation. Lv et al. identified that the chalcone synthase (CHS) and cytochrome P450 reductase (CPR) were the bottleneck for the hydroxylated flavonoid production, and optimizing the expression via adjusting the gene copy number of CHS and CPR could improve the flavonoid production [15]. In another case study, CYP450 BM3 variant was used for the biosynthesis of ERI from NAR, and the best mutant could produce 47 μ M from 100 μ M in a 3-L bioreactor [22]. Gao et al. significantly increased ERI production from NAR by adjusting promoter strength and mutating the vital enzyme flavonoid 3'-hydroxylase and its redox partner in shaking flasks, producing approximately 1 g/L of ERI from 1.5 g/L of NAR [23]. These results show that increasing the activity of enzymes or improving the expression of F3'H and F3H could lead to a boost in flavonoid synthesis.

In this study, the interaction of F3'H and redox partner cytochrome P450 reductases was optimized to improve substrate conversion, and F3'H stability in cells was improved by modifying the predicted potential ubiquitination sites. Besides, different F3Hs from different sources and different types of promoters were tested for a better performance in DHQ production in the shake flask, and the best strain could produce 381.2 ± 10.7 mg/L of DHQ from 1 g/L of NAR.

Material and methods

Strains, plasmids, and primers

All primers were synthesised by GENEWIZ (China) and Sangon Biotech (China), and are listed in Additional file 1: Table S2. The strain of *E. coli* JM109 was used for cloning purposes, and the *S. cerevisia* C800 was derived from *S. cerevisia* CEN.PK2-1D (*MAT α* , *ura3-52*, *trp1-286*, *leu2-3*, 112, *his3 Δ 1*) by inactivating the gene *gal80*, which was used for gene expression and whole-cell biocatalysis in the study. The plasmid pY26 was used for episomal expression.

Growth media and culture conditions

E. coli strains were cultivated in Erlenmeyer flasks with Luria–Bertani broth in a shaking incubator at 220 rpm and 37 °C. For plasmid construction purposes, medium should be added with a final concentration of 100 μ g/mL ampicillin to maintain plasmid stability in liquid broth or solid medium. The constructed plasmids were verified by sequencing (performed by GENEWIZ (China)) and then transformed into the yeast cells following the protocol from the literature [24]. Regarding the selection of recombinant yeast strains, yeast nitrogen base (YNB) was used to prepare the synthetic medium for isolating the auxotrophic mutants, and yeast extract peptone dextrose (YPD) was used for the cultivation of yeast cells.

Depending on the purposes, yeast were grown at 30 °C in liquid or solid medium of YNB or YPD.

Expression plasmid construction

Gene fragments were codon-optimized and synthesised by GENEWIZ (China), and assembled with the plasmid backbone from pY26-TEF-GPD [25] and pRS424 [26] following Gibson assembly. The constructed plasmids were sequenced for verification, and transformed into *S. cerevisiae* for biotransformation. The synthesised genes and constructed plasmids are listed in Additional file 1: Table S1 and Table 1.

Yeast genome edition

The yeast CRISPR/Cas9 system was used to integrate the *ScCPR* expression cassette into the genome HO site according to the protocol [27]. Briefly, sgRNA was designed based on the analysis from the CRISPR gRNA Design Tool Benchling (<https://www.benchling.com/crispr/>), and the recombination arms were fused with the *ScCPR* expression cassette, then transformed into yeast cells with CRISPR/Cas9 plasmids. Mutants were isolated from YNB-based synthetic medium without uracil for selecting yeast mutants. The mutants were counter selected on the medium containing 5-fluoroorotic acid against the *URA3* gene to remove CRISPR/Cas9 plasmids.

Biotransformation in 24 deep-well microplates

The recombinant strains were grown on YNB-URA medium, and the colonies were picked up and inoculated into 10 mL of YNB-URA liquid medium for growing at 30 °C, 220 rpm

until they reached the logarithmic phase. The 250 µL of starter was transferred to a fresh YPD medium with the addition of 1 g/L NAR as the substrate. The samples were collected after the strains had grown for 72 h at the conditions of 30 °C, 220 rpm. Similarly, the starter was prepared as mentioned before, and 30 µL of starter was transferred into 3 mL of fresh YPD medium containing 1 g/L of NAR in the 24 deep-well microplate, and samples were taken for analysis after the strain had grown for 72 h at 30 °C, 220 rpm.

Analytical methods

The optical density was determined by using a microplate reader (Tecan infinite 200 pro, Switzerland), and the samples were diluted in an appropriate range for measurement. The samples of NAR, DHQ, ERI, and DHK were mixed in an equal volume of pure methanol, and the concentrations were analysed using the Shimadzu high-performance liquid chromatography (HPLC) system (Shimadzu Corporation, Kyoto, Japan). The detection was performed using a Thermo Scientific Hypersil ODS-2 C18 column (Thermo Fisher Scientific Inc., USA), and compounds were eluted using a gradient elution protocol that consisted of acetonitrile containing 0.1% trifluoroacetic acid and water at a flow rate of 1.0 mL/min. All the compounds were detected using an ultraviolet detector A370 at 290 nm.

Table 1 The constructed plasmids for optimizing the interaction between F3'Hs and CPRs

Constructed plasmids	Characteristics	Reference
pY26- <i>SmF3'H-SmCPR</i>	Episomal expression vector, containing the genes of <i>SmF3'H</i> and <i>SmCPR</i> from <i>S. marianum</i>	This study
pY26- <i>SmF3'H-AtCPR</i>	Episomal expression vector, containing the genes of <i>SmF3'H</i> from <i>S. marianum</i> and <i>AtCPR</i> from <i>A. thaliana</i>	This study
pY26- <i>SmF3'H-EbCPR</i>	Episomal expression vector, containing the genes of <i>SmF3'H</i> from <i>S. marianum</i> and <i>EbCPR</i> from <i>E. breviscapus</i>	This study
pY26- <i>SmF3'H-GmCPR</i>	Episomal expression vector, containing the genes of <i>SmF3'H</i> from <i>S. marianum</i> and <i>GmCPR</i> from <i>G. max</i>	This study
pY26- <i>SmF3'H-HtCPR</i>	Episomal expression vector, containing the genes of <i>SmF3'H</i> from <i>S. marianum</i> and <i>HtCPR</i> from <i>H. tuberosus</i>	This study
pY26- <i>SmF3'H- HtCPR(L1M)</i>	Episomal expression vector, containing the genes of <i>SmF3'H</i> from <i>S. marianum</i> and <i>HtCPR</i> from <i>H. tuberosus</i> (replaced the start codon UUG with ATG)	This study
pY26- <i>SmF3'H- HtCPR(+ M)</i>	Episomal expression vector, containing the genes of <i>SmF3'H</i> from <i>S. marianum</i> and <i>HtCPR</i> from <i>H. tuberosus</i> (added with a start codon of ATG)	This study
pY26- <i>SmF3'H-ScCPR</i>	Episomal expression vector, containing the genes of <i>SmF3'H</i> from <i>S. marianum</i> and <i>HtCPR</i> from <i>S. cerevisiae</i>	This study
pY26- <i>FaF3'H-SmCPR</i>	Episomal expression vector, containing the genes of <i>FaF3'H</i> from <i>F. x ananassa</i> and <i>SmCPR</i> from <i>S. marianum</i>	This study
pY26- <i>FaF3'H-AtCPR</i>	Episomal expression vector, containing the genes of <i>FaF3'H</i> from <i>F. x ananassa</i> and <i>AtCPR</i> from <i>A. thaliana</i>	This study
pY26- <i>FaF3'H-EbCPR</i>	Episomal expression vector, containing the genes of <i>FaF3'H</i> from <i>F. x ananassa</i> and <i>EbCPR</i> from <i>E. breviscapus</i>	This study
pY26- <i>FaF3'H-GmCPR</i>	Episomal expression vector, containing the genes of <i>FaF3'H</i> from <i>F. x ananassa</i> and <i>GmCPR</i> from <i>G. max</i>	This study
pY26- <i>FaF3'H-HtCPR</i>	Episomal expression vector, containing the genes of <i>FaF3'H</i> from <i>F. x ananassa</i> and <i>HtCPR</i> from <i>H. tuberosus</i>	This study
pY26- <i>FaF3'H-ScCPR</i>	Episomal expression vector, containing the genes of <i>FaF3'H</i> from <i>F. x ananassa</i> and <i>ScCPR</i> from <i>S. cerevisiae</i>	This study

Results

Optimization of the expression for flavonoid 3'-hydroxylase and its redox partner

The hydroxylation of the C-ring and B-ring of flavonoids at the 3- and 3' positions, catalyzed by flavanone 3-dioxygenase (F3H) and flavonoid 3'-hydroxylase (F3'H), is required for the production of DHQ from NAR (Fig. 1A). The F3'Hs are cytochrome P450-dependent enzymes that could hydroxylate the NAR to produce ERI, and this process requires redox partners for electron delivery. Previous studies indicated that the optimization of redox partner interactions with P450 enzymes has shown faster substrate conversion and an increased product yield [28, 29], which may be achieved by optimizing of the expression F3'H and its redox partner to form a more active enzyme complex. In our study, *Silybum marianum* (*SmCPR*), *Arabidopsis thaliana* (*AtCPR*), *Erigeron breviscapus* (*EbCPR*), *Glycine max* (*GmCPR*), *Helianthus tuberosus* (*HtCPR*), and *S. cerevisiae* (*ScCPR*), and were episomally co-expressed with F3'Hs from *SmF3'H* or *Fragaria x ananassain* (*FaF3'H*) in *S. cerevisiae* (Fig. 1B and Table 1). The constructed recombinant strains were cultivated for enzyme expression in the YPD medium containing 1 g/L NAR as the substrate, and the supernatants were taken after fermentation ran for 72 h. The strains that co-expressed the *SmF3'H* and CPRs of *ScCPR*, *GmCPR*, or *SmCPR* produced much higher titres of ERI, with the best P450-reductase enzyme complex *SmF3'H/ScCPR* achieving a titre of 435.7 ± 7.6 mg/L ERI and a yield of 64.1 ± 2.2 mg/g_{CDW}, the highest titre and yield in all the experimental groups (Fig. 1C).

The truncation was applied to *SmF3'H* and *ScCPR* to investigate the influence of the transmembrane regions. The transmembrane regions of these two proteins were analyzed with the software TMHMM-2.0 and AlphaFold for structure prediction (Additional file 1: Fig. S1A), and subsequently deleted to produce the distinct truncated proteins *SmF3'H-M1*, *SmF3'H-M2*, and *ScCPR-M*. The biotransformation of NAR to ERI was not significantly impacted by the deletion of the *ScCPR*'s transmembrane region, while the truncation of *SmF3'H* nearly eliminated the catalytic activity (Additional file 1: Fig.S1B).

Improvement of the enzyme stability by mutating the potential ubiquitination sites

Ubiquitin-mediated proteasomal degradation is one of the main proteolytic pathways for regulating protein stability and turnover depending on cellular needs in eukaryotes, mainly

involving the degradation of misfolded and damaged proteins along with the short-lived proteins [30, 31]. A previous study has shown that the mutation at the sensitive ubiquitination site of *FjTAL* can lead to a substantial improvement in *p*-coumaric acid production [32]. To examine the ubiquitination sites and prolong the protein half life, an online web server for protein ubiquitination sites prediction, BDM-PUB with Bayesian Discriminant method, was used to identify the potential candidates (Table 2). These potential ubiquitination sites were mutated to arginine residues to create *SmF3'H* mutants and were episomally expressed in a *S. cerevisiae* strain that integrated a copy of *ScCPR* into the genome HO site. The recombinant strains were examined for the contribution of *SmF3'H* mutants in eriodietylol production from naringenin, and the mutant K290R was able to slightly improve *SmF3'H* performance in the conversion of NAR to ERI, obtaining a 12.8% increase in titre compared with wild type *SmF3'H* (Fig. 2). Mutations at other predicted ubiquitination sites did not improve the ERI production, and some even resulted in decreased product formation, indicating that neutral or harmful mutations occurred in the enzymes.

Selection of optimal flavanone 3-dioxygenase for dihydroquercetin production

The enzyme F3H is capable of hydroxylating the compounds on the B-rings of NAR or DHK at the 3-positions. Five different F3Hs were cloned from different plant species enriched with flavonoids and relevant compounds, including *S. marianum* (*SmF3H*), *Citrus sinensis* (*CsF3H*), *Epimedium koreanum Nakai* (*EKF3H*), *G. max* (*GmF3H*), and *Carthamus tinctorius* (*CtF3H*). To test their activities, these F3Hs were inserted into an expression vector containing F3'H and *ScCPR*, and episomally expressed under the control of P_{GAL7} in *S. cerevisiae* (Fig. 3A). After 72-h fermentation, the recombinant strain expressing *CsF3H* yielded 303.0 ± 1.7 mg/L of DHQ and a yield of 66.0 ± 3.7 mg/g_{CDW}, the highest titre and yield in all tested groups (Fig. 3B). The recombinant strain expressing *SmF3H* also showed relatively higher activities in the NAR conversion reaction, but the strain incorporating *CtF3H* showed the worst performance in producing DHQ. A small amount of the substrate NAR was detected in the supernatant, but a significant amount of intermediate metabolites were detected, including 413.3 mg/L of ± 7.8 ERI and 70.4 ± 7.2 mg/L of DHK (Fig. 3B).

(See figure on next page.)

Fig. 1 Plasmid construction and optimization of interaction between the flavonoid 3'-hydroxylase and the redox partner. **A** Schematic representation of DHQ bioproduction from NAR. **B** Plasmid construction for F3'H and CPR co-expression. **C** The tests for the optimal enzyme complex for NAR biotransformation. All the genes encoding the F3'Hs and CPR from different sources were controlled under the promoters of P_{INO1} and P_{TDH1} , respectively. For testing the expressed enzyme complex activity, one gram of NAR was used as the substrate and added to the medium YPD. All experiments were performed in triplicates and error bars indicate SD

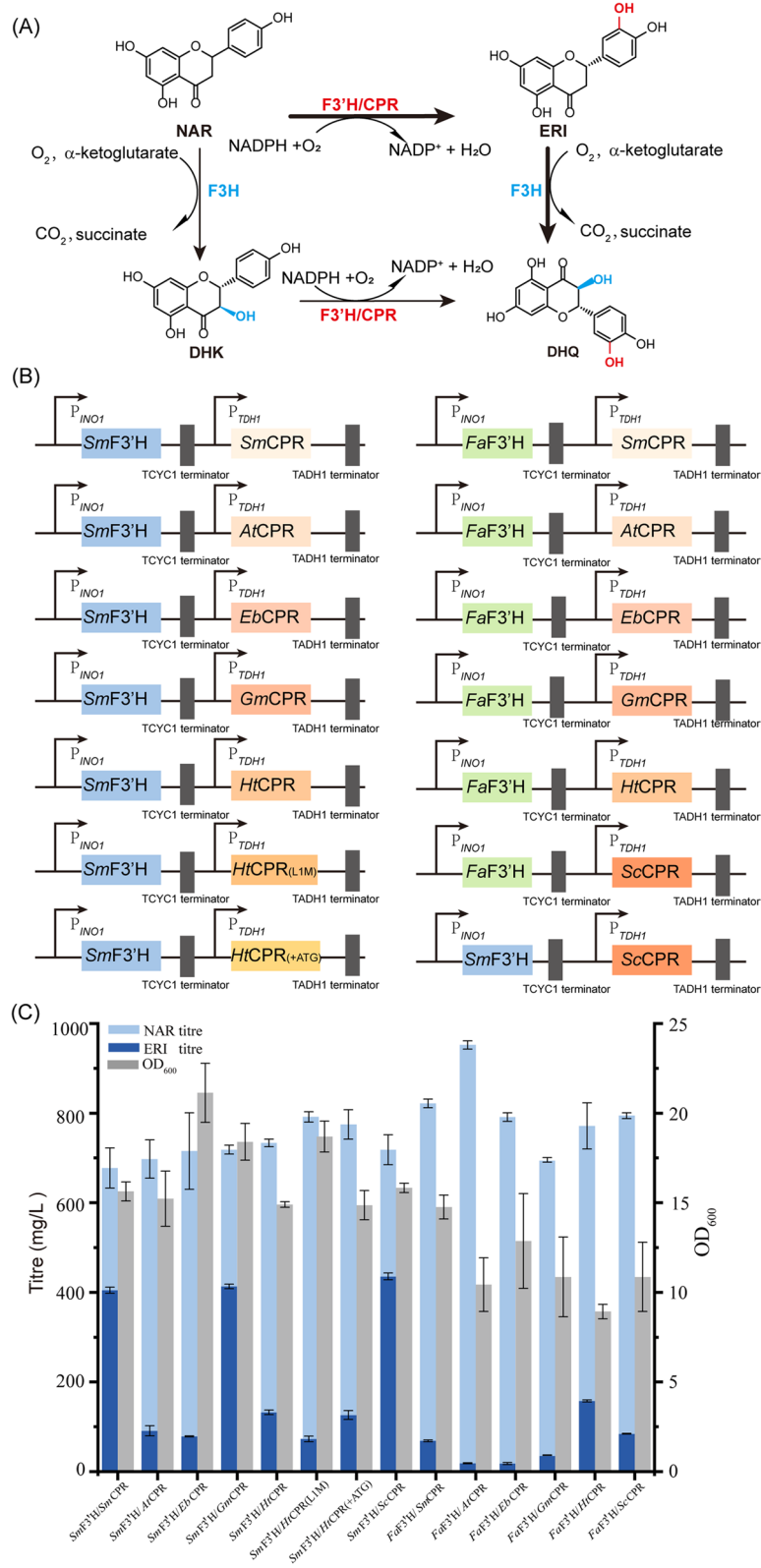


Fig. 1 (See legend on previous page.)

Table 2 The predicted ubiquitination sites on *SmF3'H*

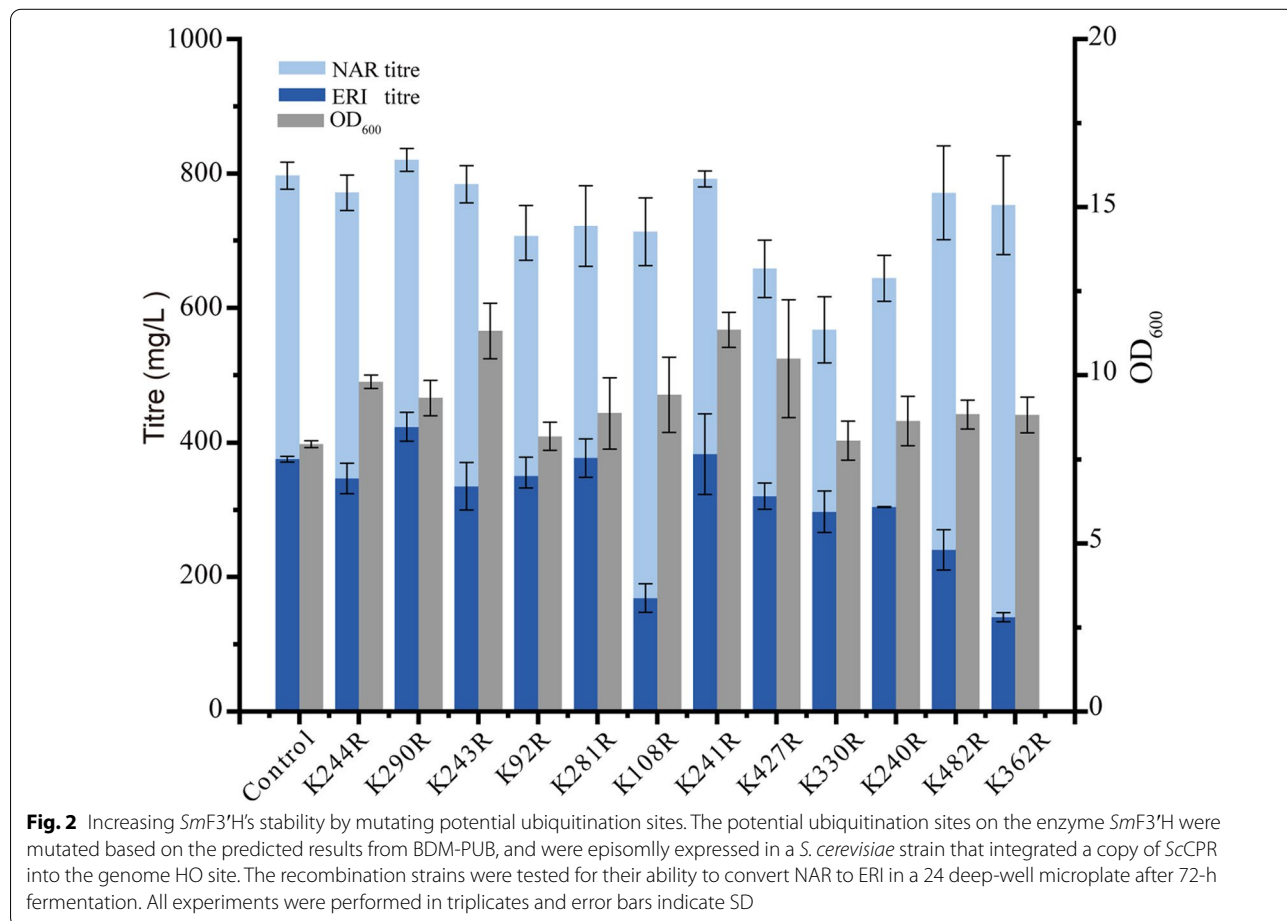
Protein	position	Sequence	scores
<i>SmF3'H</i>	244	KMK K LHL	2.13
	290	EGG K LSD	1.58
	243	KKM K LH	2.06
	92	QFL K VHD	1.90
	281	ISL K DDA	1.82
	108	SGA K HIA	1.23
	241	VT K KMK	1.08
	427	GGE K PNA	1.05
	330	QLL K QAQ	3.04
	240	SV T KMK	2.40
	482	DPE K LNM	0.51
	362	AV K ETF	2.15

The predicted ubiquitination sites were highlighted in bold

Enhancement of dihydroquercetin production by promoter adjustment

The above study showed that a considerable amount of

ERI accumulated during the NAR biotransformation, indicating the inadequate conversion of ERI to DHK. Several factors may influence F3H expression and function, such as possible interference between F3H and F3'H due to competition for limited resources in cells, promoter strength and enzyme expression variation as a result of environmental stress and pH shift [33]. Considering these possibilities, the constitutive or inducible promoters with different strengths, such as P_{SED1} , P_{TDH3} , P_{CCW12} , P_{GALI1} , P_{GAL2} , P_{GALI0} and P_{HXT7} were used to control F3H expression in *S. cerevisiae*, and episomal expression cassettes for F3H were created utilizing these promoters (Fig. 4A). The recombinant strains were conducted following the fermentation protocol described previously, and the promoter P_{GAL2} worked best in all the tested groups. The recombinant strain using P_{GAL2} for regulating the F3H expression, accumulated 381.2 ± 10.7 mg/L of DHQ from 1 g/L of NAR with a yield of 67.0 ± 6.7 mg/g_{CDW} and a conversion of 0.34 ± 0.005 mol_{DHQ}/mol_{NAR}, improving by 27.1% compared with the parental strain using the Gal7 promoter (Fig. 4B). Surprisingly, the



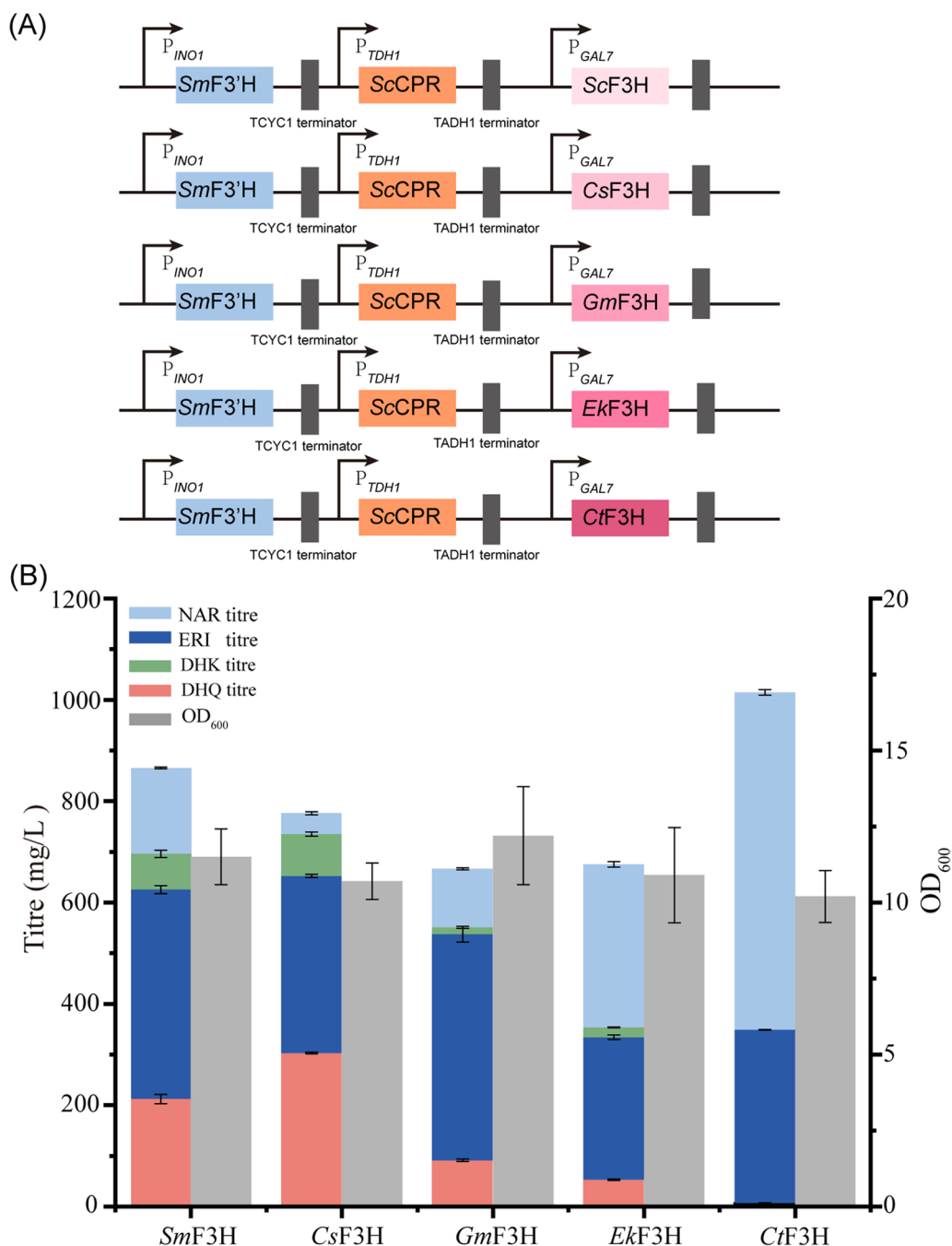
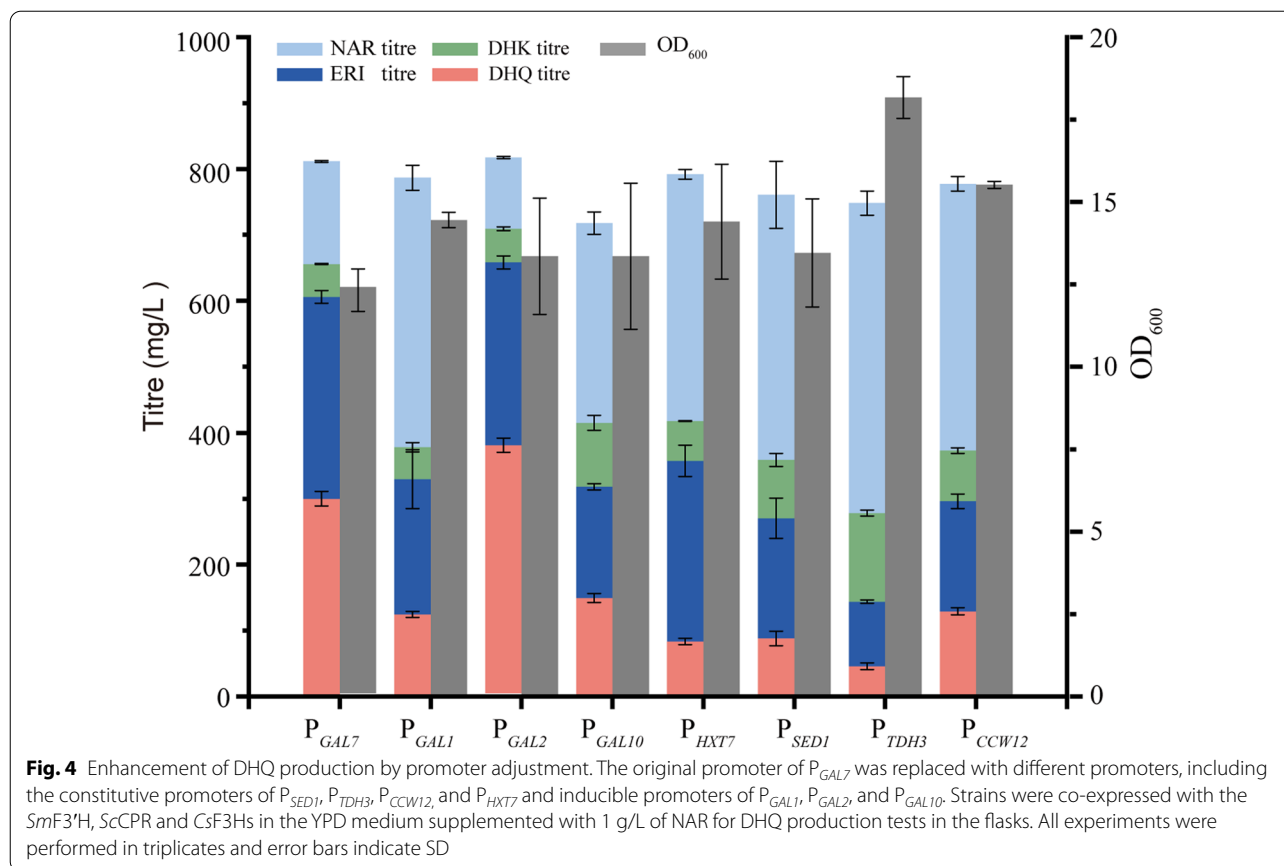


Fig. 3 Selection of optimal *F3H* for dihydroquercetin production. **(A)** Plasmid construction for the co-expression the enzymes of *F3H*s from different plant species with *SmF3'H* and *ScCPR*. The expression of *F3H*s was regulated by the inducible promoter P_{GAL7} . **(B)** Activities tests for *F3H*s by determining the NAR biotransformation in flasks. Strains were cultivated in YPD supplemented with 1 g/L of NAR as the substrate. All experiments were performed in triplicates and error bars indicate SD

strong promoters P_{SED1} , P_{TDH3} , and P_{CCW12} performed poorly in this study, and a significant amount of substrate NAR was detected, indicating interference on *F3'H* catalysis. Another interesting finding is about the using the promoter P_{HXT7} , a glucose-dependent promoter induced

at a low level of glucose, resulted in significant ERI accumulation but low DHQ formation (Fig. 4B).



Discussion

Dihydroquercetin is a bioactive flavonoid that has piqued the interest of industries and metabolic engineering communities due to its various health benefits. Dihydroquercetin bioproduction is an appealing alternative to fulfill the increased demand. Currently, DHQ has been de novo synthesized from glucose or glycerol. The titre and yield were only around 330 mg/L in *S. cerevisiae* in a bioreactor [17] and about 110 mg/L in *Y. lipolytica* at shake flask level [15]. The titre and yield are low, partly due to considerable metabolite intermediate accumulation and low efficiency in the long pathway for de novo DHQ biosynthesis, which may need deep metabolic engineering to balance modules and efficiently direct the flux for DHQ synthesis as well as reduce metabolic burdens. The high-value-added DHQ can be manufactured using the low-cost substrate NAR, extracted from fruit peel waste. Several strategies were used in this study to improve the conversion of NAR to DHQ, including optimizing the interaction between F3'H and its redox partner, increasing F3'H enzyme stability, selecting optimal F3H, and temporal regulation to the performance of two important enzymes. In addition to being a viable option for de novo DHQ bioproduction, the engineered whole-cell

biocatalyst can be applied to DHQ bioproduction by converting the relative cheap substrate NAR to value-added product.

The biosynthesis of DHQ involves hydroxylation of the flavonoid's B-ring at the 3'-position, which is catalyzed by the cytochrome P450-dependent flavonoid 3'-hydroxylase and needs the transfer of electrons to F3'H by the cytochrome P450 reductase. The P450-dependent F3'H and CPR form a 1:1 functional P450-reductase complex for the catalytic reaction, but the P450 enzyme and reductase partner may not be well balanced [34]. Furthermore, F3'H and ScCPR have been identified as membrane-bound proteins, and optimizing expression levels will allow for better use of the limited membraneous space and other bioresources for protein synthesis. Previous studies have shown that adjusting the gene copies or promoter strengths to change the relative expression levels of F3'H and CPR was effective for improving DHQ production [15, 23]. When a P450 enzyme has a higher affinity for interacting with reductase, electrons will flow to those P450s first [35]. As a result, it is envisaged that strengthening the interaction between F3'H and its reductase

partner would aid in accelerating the process. Our study demonstrated that the F3'H from *S. marianum* (*SmF3'H*) and CPR from *S. cerevisiae* (*ScCPR*) formed a functional reductase-P450 chimeric complex that performed best in the NAR conversion test. Further truncation studies revealed that the transmembrane region was critical for *SmF3'H* function maintenance, partly because the catalytic reaction needs the membrane as the matrix for interaction and reaction, and enzyme organization and function are modulated by membrane components [36, 37].

The possibility of altering the potential ubiquitination sites is another way of enhancing DHQ synthesis. This strategy increases the key enzymes' half-lives, which may help to increase protein stability and, in turn, increase the production of the target compound. In a previous study, our team showed that altering the sensitive ubiquitination site of *F/TAL* can significantly increase the synthesis of *p*-coumaric acid [32]. In this study, we conducted a test for the *SmF3'H* and mutated the sensitive ubiquitination sites, leading to a slight increase in DHQ production. However, other mutations led to a reduction in enzyme activity because they might happen in the regions where catalytic activities or interactions with redox partners occur. In addition, cells monitor and get rid of misfolded or other aberrant proteins via the ubiquitin–proteasome pathway [38, 39], and the misfolded *SmF3'H* may form aggregates and fail to be removed in time, which may cause some interference for cells. Fortunately, there is no obvious cell growth impairment that occurred in our study.

Efforts are also being undertaken to improve the activity and expression of F3H, the major enzyme responsible for hydroxylating the C-ring of flavonoids at the 3-position. Five F3Hs were selected from different plant species in our study, the F3Hs from *Petroselinum crispum* and *A. thaliana* were characterized to have significant affinity for NAR but were not chosen due to low activity in the mild pH range [40, 41]. Different types of promoters with different strengths were selected for evaluating their influence in DHQ production. Interestingly, we discovered that using strong promoters P_{SEDI} , P_{TDH3} , and P_{CCW12} [42] resulted in a significant decrease in DHQ formation, whereas several promoters related to galactose catabolism or regulation worked better than those three. This implies that *SmF3'H/CPR* expression and/or function is being interfered with. Different F3'Hs and F3Hs may exhibit a distinct variance in catalytic efficacy for diverse substrates and have different preferences for certain substrates [43]. It seems that the *SmF3'H* prefers to use the substrate NAR rather than DHK, which means the DHQ is mainly via the route of ERI converted from NAR. In this scenario, the strong constitutive expression

of F3H may compete for limited resources for *SmF3'H/CPR* expression and overwhelm cell capacity in enzyme synthesis, while the use of weak constitutive promoter P_{HXT7} does facilitate NAR conversion to ERI but with low DHQ production. To avoid such possible interference, we employed the inducible promoters of P_{GAL1} , P_{GAL2} , P_{GAL10} , and P_{GAL7} to regulate F3H expression. By combining all of these strategies, the DHQ conversion was significantly improved, compared with the previous studies.

Different strategies for strain engineering and fermentation optimization were used in the literature, resulting in DHQ production in *S. cerevisiae* at around 330 mg/L in a bioreactor after 108 h of fed-batch fermentation, three folds higher than that in a flask [17], the currently reported highest titre. In another yeast, *Y. lipolytica*, the strain was engineered to produce 110 mg/L DHQ with high intermediate accumulation in the shake flask [15]. In our study, different strategies were applied to investigate the effectiveness, which produced 381.2 mg/L DHQ from NAR in deep-well microplate. Note that a much higher density can be achieved in a bioreactor than in a deep-well microplate, probably 9–10 folds. Furthermore, the optimization of fermentation conditions can further improve DHQ production. Therefore, the engineered strain for NAR biotransformation is likely more efficient in DHQ production in our study. However, more studies should be performed in the well-controlled bioreactor for comparison in the future.

Conclusions

In conclusion, *S. cerevisiae* was engineered to produce dihydroquercetin from naringenin in this study. The key enzyme F3'H and its P450 reductase partner from different species were co-expressed in *S. cerevisiae*, and the *SmF3'H/ScCPR* formed the best P450-reductase enzyme complex to produce 435.7 ± 7.6 mg/L of ERI from NAR with a conversion rate of 0.41 ± 0.007 mol_{ERI}/mol_{NAR}. The production formation was further improved by mutating the predicted potential ubiquitination sites for enhancing the *SmF3'H* stability. Five different F3Hs from different plant species were co-expressed with *SmF3'H/ScCPR* for DHQ production, and could produced 381.2 ± 10.7 mg/L of DHQ from 1 g/L of NAR by further promoter replacement. In comparison to earlier research, the titre and yield of DHQ production was significantly improved by combining all of these strategies. This study provides systematic strategies for improving DHQ production from NAR.

Abbreviations

DHQ: Dihydroquercetin; ERI: Eriodictyol; DHK: Dihydrokaempferol; NAR: Naringenin; F3'H: Flavonoid 3'-hydroxylase; F3H: Flavanone 3-hydroxylase;

CHS: Chalcone synthase; CPR: Cytochrome P450 reductase; CRISPR: Clustered regularly interspaced short palindromic repeat.

Supplementary Information

The online version contains supplementary material available at <https://doi.org/10.1186/s12934-022-01937-8>.

Additional file 1: Table S1. Genes were synthesized in this study.
Table S2. Primers used in this study. **Fig. S1.** Influence of truncation the SmF3'H and ScCPR.

Acknowledgements

This work was supported by the National Key Research and Development Program of China (2021YFC2100700) and the Jiangsu Shuangchuang Talent Program for Mass Innovation and Entrepreneurship (JSSCBS20210847).

Author contributions

MJ, JZ, and SY, designed the research. SY wrote the manuscript; MJ performed the experiments; SY and MJ analysed and processed the data; SG and JZ reviewed the manuscript; JZ managed the project. All the authors read and approved the final manuscript.

Funding

National Key Research and Development Program of China, 2021YFC2100700; Jiangsu Shuangchuang Talent Program for Mass Innovation and Entrepreneurship, JSSCBS20210847.

Availability of data and materials

All data and materials are available as described in the study and its Additional file 1.

Declarations

Ethics approval and consent to participate

All authors read and approved the final manuscript and related ethics.

Consent for publication

All authors read and approved the final manuscript and potential publication.

Competing interests

The authors declare that they have no known competing interests.

Author details

¹Science Center for Future Foods, Jiangnan University, 1800 Lihu Road, Wuxi 214122, Jiangsu, China. ²Key Laboratory of Industrial Biotechnology, Ministry of Education and School of Biotechnology, Jiangnan University, 1800 Lihu Road, Wuxi 214122, Jiangsu, China. ³Engineering Research Center of Ministry of Education On Food Synthetic Biotechnology, Jiangnan University, 1800 Lihu Road, Wuxi 214122, Jiangsu, China. ⁴Jiangsu Province Engineering Research Center of Food Synthetic Biotechnology, Jiangnan University, 1800 Lihu Road, Wuxi 214122, Jiangsu, China.

Received: 2 August 2022 Accepted: 19 September 2022

Published online: 15 October 2022

References

- Weidmann AE. Dihydroquercetin: more than just an impurity? *Eur J Pharmacol.* 2012;684:19–26.
- Sunil C, Xu BJ. An insight into the health-promoting effects of taxifolin (dihydroquercetin). *Phytochemistry.* 2019;166:112066.
- Bernatova I, Liskova S. Mechanisms modified by (–)-epicatechin and taxifolin relevant for the treatment of hypertension and viral infection: knowledge from preclinical studies. *Antioxidants.* 2021;10:467.
- Ali SS, Ahsan H, Zia MK, Siddiqui T, Khan FH. Understanding oxidants and antioxidants: classical team with new players. *J Food Biochem.* 2020, 44.
- Das A, Baidya R, Chakraborty T, Samanta AK, Roy S. Pharmacological basis and new insights of taxifolin: a comprehensive review. *Biomed Pharmacother.* 2021;142:112004.
- Jo S, Kim S, Shin DH, Kim M-S. Inhibition of SARS-CoV 3CL protease by flavonoids. *J Enzyme Inhib Med Chem.* 2020;35:145–51.
- Adhikari B, Marasini BP, Rayamajhee B, Bhattarai BR, Lamichhane G, Khadayat K, Adhikari A, Khanal S, Parajuli N. Potential roles of medicinal plants for the treatment of viral diseases focusing on COVID-19: a review. *Phytother Res.* 2021;35:1298–312.
- Qiu XL, Zhang QF. Acidic hydrolysis of astilbin and its application for the preparation of taxifolin from *Rhizoma Smilacis Glabrae*. *J Chem Res.* 2021;45:290–4.
- Wallace SN, Carrier DJ, Clausen EC. Batch solvent extraction of flavanolignans from milk thistle (*Silybum marianum* L. Gaertner). *Phytochem Anal.* 2005;16:7–16.
- Ma CH, Yang L, Wang WJ, Yang FJ, Zhao CJ, Zu YG. Extraction of dihydroquercetin from *Larix gmelinii* with ultrasound-assisted and microwave-assisted alternant digestion. *Int J Mol Sci.* 2012;13:8789–804.
- Macha L, Dorigundla AR, Gurrapu R, Vanka US, Batchu VR. Total synthesis of the natural products ulmoside A and (2R,3R)-taxifolin-6-C-β-d-glucopyranoside. *Synlett.* 2020;31:1097–101.
- Khan AY, Preskorn SH, Wimalasena K. Single enantiomer drugs: should they be developed? *Essent Psychopharmacol.* 2006;7:15–23.
- Andersson T. Single-isomer drugs: true therapeutic advances. *Clin Pharmacokinet.* 2004;43:279–85.
- Kandemir K, Piskin E, Xiao J, Tomas M, Capanoglu E. Fruit juice industry wastes as a source of bioactives. *J Agric Food Chem.* 2022;70:6805–32.
- Lv Y, Marsafari M, Koffas M, Zhou J, Xu P. Optimizing oleaginous yeast cell factories for flavonoids and hydroxylated flavonoids biosynthesis. *ACS Synth Biol.* 2019;8:2514–23.
- Park SY, Yang D, Ha SH, Lee SY. Production of phenylpropanoids and flavonolignans from glycerol by metabolically engineered *Escherichia coli*. *Biotechnol Bioeng.* 2022;119:946–62.
- Yang J, Liang J, Shao L, Liu L, Gao K, Zhang J-L, Sun Z, Xu W, Lin P, Yu R, Zi J. Green production of silybin and isosilybin by merging metabolic engineering approaches and enzymatic catalysis. *Metab Eng.* 2020;59:44–52.
- Han Y, Huang K, Liu Y, Jiao T, Ma G, Qian Y, Wang P, Dai X, Gao L, Xia T. Functional analysis of two flavanone-3-hydroxylase genes from *Camellia sinensis*: a critical role in flavonoid accumulation. *Genes.* 2017;8:300.
- Hammerbacher A, Kandasamy D, Ullah C, Schmidt A, Wright LP, Gershenzon J. Flavanone-3-hydroxylase plays an important role in the biosynthesis of spruce phenolic defenses against bark beetles and their fungal associates. *Front Plant Sci.* 2019;10:208–208.
- Brugliera F, Barri-Rewell G, Holton TA, Mason JG. Isolation and characterization of a flavonoid 3'-hydroxylase cDNA clone corresponding to the Ht1 locus of *Petunia hybrida*. *Plant J.* 1999;19:441–51.
- Baba SA, Ashraf N. Functional characterization of flavonoid 3'-hydroxylase, Csf3'H, from *Crocus sativus* L: Insights into substrate specificity and role in abiotic stress. *Arch Biochem Biophys.* 2019;667:70–8.
- Chu LL, Pandey RP, Jung N, Jung HJ, Kim E-H, Sohng JK. Hydroxylation of diverse flavonoids by CYP450 BM3 variants: biosynthesis of eriodictyol from naringenin in whole cells and its biological activities. *Microb Cell Fact.* 2016;15:135.
- Gao S, Xu XY, Zeng WZ, Xu S, Lyv YB, Feng Y, Kai GY, Zhou JW, Chen J. Efficient biosynthesis of (2S)-eriodictyol from (2S)-naringenin in *Saccharomyces cerevisiae* through a combination of promoter adjustment and directed evolution. *ACS Synth Biol.* 2020;9:3288–97.
- Gietz RD, Schiestl RH. High-efficiency yeast transformation using the LiAc/SS carrier DNA/PEG method. *Nat Protoc.* 2007;2:31–4.
- Li A, Liu Z, Li Q, Yu L, Wang D, Deng X. Construction and characterization of bidirectional expression vectors in *Saccharomyces cerevisiae*. *FEMS Yeast Res.* 2008;8:6–9.
- Gao S, Lyu Y, Zeng W, Du G, Zhou J, Chen J. Efficient Biosynthesis of (2S)-Naringenin from p-Coumaric Acid in *Saccharomyces cerevisiae*. *J Agric Food Chem.* 2020;68:1015–21.
- Mans R, van Rossum HM, Wijsman M, Backx A, Kuijpers NGA, van den Broek M, Daran-Lapujade P, Pronk JT, van Maris AJA, Daran JMG. CRISPR/Cas9: a molecular Swiss army knife for simultaneous introduction of multiple genetic modifications in *Saccharomyces cerevisiae*. *FEMS Yeast Res.* 2015, 15.

28. Sagadin T, Riehm JL, Milhim M, Hutter MC, Bernhardt R. Binding modes of CYP106A2 redox partners determine differences in progesterone hydroxylation product patterns. *Commun Biol*. 2018;1:99.
29. Biggs BW, Lim CG, Sagliani K, Shankar S, Stephanopoulos G, De Mey M, Ajikumar PK. Overcoming heterologous protein interdependency to optimize P450-mediated Taxol precursor synthesis in *Escherichia coli*. *Proc Natl Acad Sci USA*. 2016;113:3209–14.
30. Komander D, Rape M. The ubiquitin code. *Annu Rev Biochem*. 2012;81:203–29.
31. Zattas D, Hochstrasser M. Ubiquitin-dependent protein degradation at the yeast endoplasmic reticulum and nuclear envelope. *Crit Rev Biochem Mol Biol*. 2015;50:1–17.
32. Mingjia Li JZ, Li Jianghua. Effect of key enzymes ubiquitination sites on the biosynthesis of naringenin. *Chin J Biotechnol*. 2022;38:691–704.
33. Weinhandl K, Winkler M, Glieder A, Camattari A. Carbon source dependent promoters in yeasts. *Microb Cell Fact*. 2014;13:5.
34. Barnaba C, Taylor E, Brozik JA. Dissociation constants of cytochrome P450 2C9/cytochrome P450 reductase complexes in a lipid bilayer membrane depend on NADPH: a single-protein tracking study. *J Am Chem Soc*. 2017;139:17923–34.
35. Backes WL, Kelley RW. Organization of multiple cytochrome P450s with NADPH-cytochrome P450 reductase in membranes. *Pharmacol Ther*. 2003;98:221–33.
36. Zhang M, Huang R, Im S-C, Waskell L, Ramamoorthy A. Effects of membrane mimetics on cytochrome P450-cytochrome *b5* interactions characterized by NMR spectroscopy *. *J Biol Chem*. 2015;290:12705–18.
37. Brignac-Huber LM, Park JW, Reed JR, Backes WL. Cytochrome P450 organization and function are modulated by endoplasmic reticulum phospholipid heterogeneity. *Drug Metab Dispos*. 2016;44:1859–66.
38. Berner N, Reutter K-R, Wolf DH. Protein quality control of the endoplasmic reticulum and ubiquitin–proteasome-triggered degradation of aberrant proteins: yeast pioneers the path. *Annu Rev Biochem*. 2018;87:751–82.
39. Roos-Mattjus P, Sistonen L. The ubiquitin-proteasome pathway. *Ann Med*. 2004;36:285–95.
40. Owens DK, Crosby KC, Runac J, Howard BA, Winkel BSJ. Biochemical and genetic characterization of *Arabidopsis* flavanone 3 β -hydroxylase. *Plant Physiol Biochem*. 2008;46:833–43.
41. Britsch L. Purification and characterization of flavone synthase I, a 2-oxoglutarate-dependent desaturase. *Arch Biochem Biophys*. 1990;282:152–60.
42. Gao S, Zhou H, Zhou J, Chen J. Promoter-library-based pathway optimization for efficient (2S)-naringenin production from *p*-coumaric acid in *Saccharomyces cerevisiae*. *J Agric Food Chem*. 2020;68:6884–91.
43. Park S, Choi MJ, Lee JY, Kim JK, Ha SH, Lim SH. Molecular and biochemical analysis of two rice flavonoid 3'-hydroxylase to evaluate their roles in flavonoid biosynthesis in rice grain. *Int J Mol Sci*. 2016;17:1549.

Publisher's Note

Springer Nature remains neutral with regard to jurisdictional claims in published maps and institutional affiliations.

Ready to submit your research? Choose BMC and benefit from:

- fast, convenient online submission
- thorough peer review by experienced researchers in your field
- rapid publication on acceptance
- support for research data, including large and complex data types
- gold Open Access which fosters wider collaboration and increased citations
- maximum visibility for your research: over 100M website views per year

At BMC, research is always in progress.

Learn more biomedcentral.com/submissions

